

This discussion paper is/has been under review for the journal *Climate of the Past* (CP).
Please refer to the corresponding final paper in CP if available.

Pollen-based temperature and precipitation inferences for the montane forest of Mt. Kilimanjaro during the last Glacial and the Holocene

L. Schüler^{1,2}, A. Hemp¹, and H. Behling²

¹Department of Plant Systematics, University of Bayreuth, Bayreuth, Germany

²Department of Palynology and Climate Dynamics, University of Göttingen, Göttingen, Germany

Received: 11 December 2013 – Accepted: 29 December 2013 – Published: 15 January 2014

Correspondence to: L. Schüler (lisa.schueler@uni-bayreuth.de)

Published by Copernicus Publications on behalf of the European Geosciences Union.

[Title Page](#)

[Abstract](#)

[Introduction](#)

[Conclusions](#)

[References](#)

[Tables](#)

[Figures](#)

[⏪](#)

[⏩](#)

[◀](#)

[▶](#)

[Back](#)

[Close](#)

[Full Screen / Esc](#)

[Printer-friendly Version](#)

[Interactive Discussion](#)

Abstract

The relationship between modern pollen-rain taxa and measured climate variables was explored along the elevational gradient of the southern slope of Mt. Kilimanjaro, Tanzania. Pollen assemblages in 28 pollen traps positioned on 14 montane forest vegetation plots were identified and their relationship with climate variables was examined using multivariate statistical methods. Canonical correspondence analysis revealed that the mean annual temperature, mean annual precipitation and minimum temperature each account for significant fractions of the variation in pollen taxa. A training set of 107 modern pollen taxa was used to derive temperature and precipitation transfer functions based on pollen subsets using weighted-averaging-partial-least-squares (WA-PLS) techniques. The transfer functions were then applied to a fossil pollen record from the montane forest of Mt. Kilimanjaro and the climate parameter estimates for the Late Glacial and the Holocene on Mt. Kilimanjaro were inferred. Our results present the first quantitatively reconstructed temperature and precipitation estimates for Mt Kilimanjaro and give highly interesting insights into the past 45 000 yr of climate dynamics in tropical East Africa. The climate reconstructions are consistent with the interpretation of pollen data in terms of vegetation and climate history of afro-montane forest in East Africa. Minimum temperatures above the frostline as well as increased precipitation turn out to be crucial for the development and expansion of montane forest during the Holocene. In contrast, consistently low minimum temperatures as well as about 25 % drier climate conditions prevailed during the pre LGM, which kept the montane vegetation composition in a stable state.

In prospective studies, the quantitative climate reconstruction will be improved by additional modern pollen rain data, especially from lower elevations with submontane dry forests and colline savanna vegetation in order to extend the reference climate gradient.

Pollen-based temperature and precipitation inferences

L. Schüler et al.

[Title Page](#)

[Abstract](#)

[Introduction](#)

[Conclusions](#)

[References](#)

[Tables](#)

[Figures](#)



[Back](#)

[Close](#)

[Full Screen / Esc](#)

[Printer-friendly Version](#)

[Interactive Discussion](#)



1 Introduction

Many environmental issues, like global warming or altered precipitation patterns, have increased the interest in fossil species assemblages as indicator of the palaeo-environment. In palaeoecology the direct measurement of environmental variables is impossible; consequently there is the need to resort to indirect methods. Fossil taxa assemblages can provide a record of the palaeoenvironment since each biological species requires particular environmental conditions for regeneration, establishment and growth. Today, this principle idea is primarily used in biomonitoring (Spellerberg, 1991). Nevertheless, it is also possible to infer the past environmental conditions at a site from the species composition that occurred there. Fossil taxa records are valuable for obtaining a historical perspective of current environmental problems such as acid rain (Battarbee, 1984) and global warming (Fritz et al., 1991; Walker et al., 1991).

The earliest attempt to quantitatively reconstruct past climate using pollen data was the use of indicator taxa in pollen records (Conolly, 1961; Zagwijn, 1960, 1994; Faegri and Iversen, 1989). Several numerical procedures for quantitatively reconstructing past environments from fossil pollen assemblages have been developed in the past decades; these include transfer functions (Imbrie and Kipp, 1971; Bartlein et al., 1984), pollen response surface (Bartlein et al., 1986; Prentice et al., 1991), modern analogue technique (Nakagawa et al., 2002; Overpeck et al., 1985; Guiot, 1990), and weighted averaging (Birks, 1995, 1998; Birks et al., 1990; ter Braak and Juggins, 1993; Li et al., 2007; Jongman et al., 1995). Such techniques have been widely applied to many palaeo-records worldwide, such as Europe (Huntley and Prentice, 1988; Guiot et al., 1989; Birks, 1995; Seppä et al., 2004), Asia (Xu et al., 2009; Li et al., 2007; Nakagawa et al., 2002), America (Webb III and Bryson, 1972; Markgraf et al., 2002) and also Africa (Bonnefille and Chalié, 2000; Cheddadi et al., 1998). Webb and Bryson (1972), who were the first to develop transfer function for the pollen assemblage in lake sediments, developed their transfer function based only on 8 pollen types since they excluded many pollen types for a variety of reasons (local origin, function of human

CPD

10, 195–234, 2014

Pollen-based temperature and precipitation inferences

L. Schüler et al.

Title Page

Abstract

Introduction

Conclusions

References

Tables

Figures



Back

Close

Full Screen / Esc

Printer-friendly Version

Interactive Discussion



Pollen-based temperature and precipitation inferences

L. Schüler et al.

[Title Page](#)

[Abstract](#)

[Introduction](#)

[Conclusions](#)

[References](#)

[Tables](#)

[Figures](#)

[⏪](#)

[⏩](#)

[◀](#)

[▶](#)

[Back](#)

[Close](#)

[Full Screen / Esc](#)

[Printer-friendly Version](#)

[Interactive Discussion](#)

These recent advances in quantitative environmental reconstruction procedures now allow palaeoecologists to explore many critical ecological questions, answers to which require the unique long-term temporal perspective provided by palaeoecology. What are the rates of change in ecological processes? Which processes result in given ecological thresholds being crossed, or resilience? Did novel systems, non-analogue systems, occur in the past and which combination of factors did lead to such systems (Willis et al., 2010a)? Answers to these questions (Froyd and Willis, 2008; Willis et al., 2010b; Macdonald et al., 2008) highlight the contributions that palaeoecological reconstruction can make in understanding ecological and evolutionary processes responsible for biodiversity patterns (Birks et al., 2010).

The central assumption in plant ecology is that climate has the dominant control on the distribution of the major vegetation types of the world. The climate space required to describe taxa distributions requires at least two dimensions related to temperature and water availability because of the existence of bioclimatic limits on the distribution of taxa (Woodward and Williams, 1987; Harrison et al., 2010). At the global scale responses to extreme minimum temperatures and to the hydrological budget predict the distribution limits of the major vegetation (Woodward and Williams, 1987). Further, frost stress plays a decisive role in plant distribution since it serves as a very selective filter and operates over very long time scales (Larcher and Bauer, 1981; Sakai and Larcher, 1987). Hence, the composition of natural vegetation in an area is also adjusted to local low temperature extremes (Körner, 2003).

Fossil pollen records provide evidence of changing plant compositions through time (Pickett et al., 2004; Marchant et al., 2009; Prentice et al., 2000). Pollen can often be identified to genus and family level, but only rarely to species level. Higher taxa levels tend to have distributions as coherent as lower taxa or species in climate space (Wake et al., 2009; Huntley et al., 1989). Bioclimatic limits determine the fundamental niche of taxa, but niches of taxa, especially at higher level, commonly overlap. They also vary in abundance; either with maximum values near physiological optima, or displaced by competition. Therefore more-or-less continuous variation in taxa abundance

along environmental gradients in space are found, and we can establish relationships between taxa composition and climate parameter space (Jackson and Williams, 2004).

This present study aims at the development of an ecologically plausible and significant transfer functions through the calibration of the relationships between modern pollen assemblages, vegetation belts and several ecologically determinant climate parameters such as mean annual temperature (MAT), mean annual precipitation (MAP) and minimum temperature (Tmin) in the Kilimanjaro area. The transfer functions are then applied to the fossil WeruWeru 26 pollen record from 2600 ma.s.l. on the SE slope of Mt. Kilimanjaro to reconstruct the past vegetation and climate dynamics of equatorial East Africa of the past about 50 kyrBP.

2 Study site

Mt. Kilimanjaro is a relict of an ancient volcano, which was formed as part of the East African Rift Zone. It is located at the border to Kenya 300 km south of the equator in Tanzania and about 300 km west of the Indian Ocean (Fig. 1a). It rises from savanna plains at 700 m up to its glaciated summit at 5895 m a.s.l.

2.1 Vegetation

Mt. Kilimanjaro has several different bioclimatic zones (Fig. 1b and c): the dry and hot colline savanna zone surrounds the mountain base between 700 and 1100 ma.s.l. Most of this area is used for crop production (maize, beans and sunflowers) or as meadows. Remnants of the former savanna woodlands (*Acacia*, *Terminalia*, *Grewia*, and *Combretum*) are encountered mainly around Lake Chala in the eastern foothills and on the northwestern side of the mountain. The submontane and lower montane forest belts between 1000 and 1800 m have been converted to coffee-banana fields, a special type of agroforestry called “Chagga home gardens”. Remnants of the former forests of this belt (*Newtonia*, *Strombosia* and *Entandrophragma*) are mainly restricted

CPD

10, 195–234, 2014

Pollen-based temperature and precipitation inferences

L. Schüler et al.

Title Page

Abstract

Introduction

Conclusions

References

Tables

Figures

⏪

⏩

◀

▶

Back

Close

Full Screen / Esc

Printer-friendly Version

Interactive Discussion



at the summit (Kibo, 5895 ma.s.l.) (Thompson et al., 2002). Temperature lapse rates vary from 0.51 to 0.56 °C per 100 m elevation (Hemp, 2006b). Frost occurs from 2700 m upwards (Hemp, 2006a).

3 Material and method

3.1 The pollen record

In total 76 samples were taken every 2 cm from a 165 cm long WeruWeru 26 (WW26) sediment core. The core was obtained from a soil pit by hammering five 50 cm long zinc metal cases consecutively into the pit wall. Due to the high content of un-decomposed material it was only possible to extract sediment from 15 cm below the soil surface downwards. The material was wrapped into plastic foil and kept under cool and dark conditions until transported back to the University of Göttingen. For pollen analysis a sample volume of 0.5 cm³ was prepared in the lab applying the standard method (Faegri and Iversen, 1989). The extracted pollen samples were mounted in glycerine jelly for pollen identification and counting.

The chronology is based on 13 AMS dated samples (see Supplement); 11 samples were dated at the Physical Institute of the University Erlangen-Nuremberg/Germany and two samples by Beta Analytic in Miami, Florida/USA. According to the results, samples from 17 to 52 cm core depth can be assigned to the Holocene. Samples between 66 and 165 cm core depth belong to the Late Pleistocene. There was no pollen in the sediment below 123 cm depth.

3.2 Modern pollen-rain data

The pollen and climate data sets used for the training data set included the 14 plots of the WeruWeru transect on the southern slope of Kilimanjaro. The modern pollen-rain was captured in pollen traps installed on 14 montane forest plots every 100 m elevation between 1900 and 3200 ma.s.l. On each plot the rainfall was recorded using dipping

Pollen-based temperature and precipitation inferences

L. Schüler et al.

Title Page

Abstract

Introduction

Conclusions

References

Tables

Figures

⏪

⏩

◀

▶

Back

Close

Full Screen / Esc

Printer-friendly Version

Interactive Discussion



Pollen-based temperature and precipitation inferences

L. Schüler et al.

[Title Page](#)

[Abstract](#)

[Introduction](#)

[Conclusions](#)

[References](#)

[Tables](#)

[Figures](#)

[⏪](#)

[⏩](#)

[◀](#)

[▶](#)

[Back](#)

[Close](#)

[Full Screen / Esc](#)

[Printer-friendly Version](#)

[Interactive Discussion](#)



This ordination method is preferably applied to data of species abundance and relative frequency that have a large number of zero values (Legendre and Legendre, 2012). DCAs and CCAs were carried out using CANOCO 4.54 (ter Braak and Šmilauer, 1997; 2002) and summarized in Table 2.

5 Forward selection was used to select a subset of the explanatory pollen taxa for each climate variable individually so that each pollen taxa present in the subset specifically contributes to the explanatory power of the subset. Pollen taxa with a contribution of $\geq 20\%$, representing the percentage contribution of the particular taxa to the explanatory power of the whole subset of taxa, were selected (Table 3).

10 3.4 WAPLS climate reconstruction and assessment of model performance

For the climate variables MAP, MAT and Tmin, pollen-based inference models were developed using weighted-averaging-partial-least-squares (WAPLS) models (ter Braak and Juggins, 1993). The WA-PLS procedure and the reconstruction was computed using the program R and the “rioja” package (Juggins, 2012). In applications like the present one, large test sets are not available; instead the prediction errors are simulated by bootstrap cross-validation (number of boot cycles: 1000). The goal of bootstrapping is to assign measures of accuracy to sample estimates.

15 Since it is not easily possible to quantitatively estimate to what degree pollen taxa abundance represents rather a function of local origin and/or pollen under- or over-representation, three WA-PLS calibration functions were developed, each on non-transformed and transformed species subsets (as selected by forward selection for each climate variable) for a comparison. Finally, the models were used to reconstruct MAP, MAT and Tmin based on the WW26 pollen data set. The root-mean-square error of prediction (RMSEP) is a frequently used measure of the differences between values predicted by a model and the values observed. Further, checking the predictive worth of an environmental model includes a goodness of fit metric (R^2) to quantify the degree of matching to recorded data, thereby giving a measure of model performance. Standard goodness-of-fit statistics as R^2 are an appropriate measure for model evaluation

(Guiot and Vernal, 2007). A randomized t test was used to test the significance level of the WAPLS components. Subsequently, the significant WAPLS components were used for the transfer-functions. Error bars indicate the standard error of bootstrap climate parameter estimates.

5 A principle component analysis (PCA) was performed on the fossil pollen data set of WW26 to derive main trends in vegetation change over time. The data set was square root transformed prior to the ordination to reduce the effects of over-represented taxa in the pollen record.

4 Results

10 4.1 MAP, MAT and Tmin along the WeruWeru transect

Figure 2 shows the trend of MAP, MAT and Tmin along the elevational gradient between 1900 and 3200 m a.s.l. of the southern slope of Mt. Kilimanjaro. Starting off with 2750 mm (at 1900 m a.s.l.) the MAP peaks at 2300 m elevation with about 3450 mm rainfall. It then gradually decreases with increasing elevation to 1600 mm at 3200 m a.s.l. MAT (Fig. 2b) shows a linear decrease in temperature uphill. While the MAT reaches 14.2 °C at 1900 m a.s.l., it drops to 7.06 °C at 3200 m a.s.l.

15 Tmin of the recorded time period shows a linearly decreasing trend with increasing elevation (Fig. 2c). At 1900 m a.s.l., the lowest temperature recorded was 6.01 °C. A Tmin of -1.2 °C was recorded at 3200 m a.s.l. The frost line is crossed at about 2840 m a.s.l. as suggested by interpolation of the local regression function. However, 20 temperatures below zero were also recorded at 2700 m a.s.l.

4.2 Pollen taxa response to MAP, MAT and Tmin gradients

In Fig. 3 the response functions of several representative pollen taxa (*Araliaceae*, *Olea*, *Macaranga* and *Podocarpus*) to MAP, MAT and Tmin are depicted.

Pollen-based temperature and precipitation inferences

L. Schüler et al.

Title Page

Abstract

Introduction

Conclusions

References

Tables

Figures

⏪

⏩

◀

▶

Back

Close

Full Screen / Esc

Printer-friendly Version

Interactive Discussion



Pollen-based temperature and precipitation inferences

L. Schüler et al.

[Title Page](#)

[Abstract](#)

[Introduction](#)

[Conclusions](#)

[References](#)

[Tables](#)

[Figures](#)

[⏪](#)

[⏩](#)

[◀](#)

[▶](#)

[Back](#)

[Close](#)

[Full Screen / Esc](#)

[Printer-friendly Version](#)

[Interactive Discussion](#)

Araliaceae pollen grains are most abundant at site with 2090 mm and at 2220 mm MAP (23 % of the recorded pollen sum and 18 % respectively) (Fig. 3a). Lowest abundance values are recorded at sites with annual rainfall of 1610 to 1830 mm and with MAP > 2900 mm. Despite the strong variation of abundance, Araliaceae pollen shows a unimodal response to MAP with an optimum abundance at sites with 1800 to 2400 mm of rainfall. *Olea* pollen has the highest abundance at 1930 mm MAP. At lower and higher precipitation, the abundance decreases gradually. *Macaranga* pollen grains show an abundance of about 5 to 15 % at every site (MAP range: 1600 to 3450 mm) except for three: at locations with 3670, 2920 and 2750 mm MAP this pollen taxon is very abundant (70 to 75 %). *Podocarpus* pollen grains show a unimodal response to MAP with highest abundance of 43 % at 2210 mm of rainfall. The abundance decreases gradually with higher and lower MAP.

The MAT plot (Fig. 3b) shows that Araliaceae pollen grains are abundantly recorded (18 to 24 %) at sites ranging from 8.5 to 11.0 °C MAT. At sites with higher or lower MAT the abundance of Araliaceae pollen is < 2.5 %. *Olea* pollen grains are most abundant (0.3 to 1.4 %) between 7 and 10.5 °C. Then, with increasing MAT (> 11 °C), *Olea* decreases and is not recorded at sites with MAT > 12.6 °C. *Macaranga* pollen grains show an abundance of about 5 to 15 % at every sites with MAT < 12 °C. Between 12 and 14.3 °C this pollen taxon is very abundant (70 to 75 %). *Podocarpus* pollen grains are not very common at sites with MAT < 9 °C (< 9 %). They are most abundant between 9 and 11 °C and then the record of *Podocarpus* pollen decreases with increasing MAT.

The response function of the pollen taxa to T_{min} is very much alike the one observed from MAT.

4.3 Multivariate analyses of the modern pollen-rain and subset selection

The Detrended Correspondence Analysis (DCA) of the untransformed modern pollen-rain data revealed a length of environmental gradient of 2.49 inherit in the data. This result and the predominantly unimodal response of single pollen taxa suggested to

continue with a Canonical Correspondence Analysis (CCA, a unimodal based constrained ordination).

The CCA triplots (Fig. 4a and b) represent simultaneously the ordination of samples (sites labelled with elevation in m.a.s.l.), pollen taxa (30 % best fit) and their relationship to climate variables. In the ordination diagrams, the climate variables (MAP, MAT, Tmin) are represented by vectors, the point of direction indicates increasing values of the respective parameter.

The proximity of pollen taxa and sites to any climate parameter can be interpreted as a relative measure for the correlation between those data point. Sites that a closer positioned to climate variable vector respectively, experience higher temperature or precipitation. Taxa that show a positive correlation with either of the climate parameters are most abundant at sites with high values of this parameter.

Hagenia and *Erica* pollen grains are negatively correlated with all three climate parameters whereas *Macaranga* shows a positive correlation. *Ilex* is more strongly correlated with MAP than with MAT, the opposite is the case for *Podocarpus* pollen grains, which are slightly more correlated with MAT. Taxa that are positioned close to the centre of the ordination diagram do either not show a clear linear relationship with any climate variable, show a unimodal response and/or do not significantly contribute to the variance of the whole data set (hence, the dispersion of taxa within the ordination space).

The summary of the CCA (Table 1) shows that the first two CCA axes with MAP as single constraining variable accounted for 33.46 % of the cumulative variance in the pollen data. For the MAT the first two CCA axes account for 34.52 %, for Tmin this is 34.92 %. Pseudo-canonical correlation between pollen taxa and the climate variable is 0.943 for MAP, 0.9616 for MAT and 0.9665 for Tmin. The Monte Carlo permutation test results reveal high significance levels for all three climate parameters ($p = 0.002$).

The forward selection revealed 24 pollen taxa with an explanatory contribution $\geq 20\%$ for MAP, 25 taxa for MAT and 15 taxa for Tmin (Table 2).

Pollen-based temperature and precipitation inferences

L. Schüler et al.

Title Page

Abstract

Introduction

Conclusions

References

Tables

Figures



Back

Close

Full Screen / Esc

Printer-friendly Version

Interactive Discussion



4.4 Model performance and climate reconstruction of the WW26 pollen record using Weighted-Averaging Least Square Regression (WA-PLS)

The model performance is summarized by several measures (Table 3). The performance of the WA-PLS is expressed by the Root Mean Square Error (RMSEP) of the climate parameter models, based on square-root transformed training subsets. RMSEPs are not standardized but values are expressed in terms of the original variables. The randomized t test results reveal that for MAP, MAT and Tmin only the first WA-PLS component ($p < 0.001$) is significant. Hence, these components were used for the transfer-functions. R^2 refers to the “fraction of variance explained” by the model; the R^2 values for MAP, MAT and Tmin reveal a close relationship between the bootstrap cross validated reconstructed and modern climate variables. The error bars indicate the standard error of bootstrap estimated climate parameters of the correspondent WA-PLS component.

Due to sediment loss (hiatus), the palaeosoil sequence between 56 and 66 cm the Last Glacial Maximum (LGM) is missing. According to the AMS chronology the sequence above the hiatus (< 56 cm depth) is made up of mid to late Holocene sediment (ca. 6 to 0 kyrBP) and the sediment below the hiatus (> 66 cm depth) belongs to the mid Last Glacial (ca. 46 to 36 kyrBP).

Earlier than 44 kyrBP our model reconstructs a MAP is between 1530 and 1620 mm. It then reaches a temporary high around 42 kyrBP (around 90 cm depth, above 1680 mm) and then drops back to 1550 mm soon after (at 85 cm depth). The remaining time prior to 36 kyrBP MAP fluctuates between 1670 and 1550 mm. In the mid Holocene, just before 6 kyrBP, our model reconstructs similar MAP values as for the late Last Glacial (ca. 1650 mm). Between 6.1 and 2.6 kyrBP MAP increases rapidly up to 1940 mm. Maximum MAP (1950 mm) is reached in the late Holocene at about 1.9 kyrBP (29 cm depth). 2030 mm are reconstructed for the modern pollen rain sample at the study site at 2600 m.a.s.l., which very close to the observed precipitation from

Pollen-based temperature and precipitation inferences

L. Schüler et al.

[Title Page](#)

[Abstract](#)

[Introduction](#)

[Conclusions](#)

[References](#)

[Tables](#)

[Figures](#)

[⏪](#)

[⏩](#)

[◀](#)

[▶](#)

[Back](#)

[Close](#)

[Full Screen / Esc](#)

[Printer-friendly Version](#)

[Interactive Discussion](#)



the site (2077 mm). The lowest MAP of 1530 mm is reconstructed for about 45 kyrBP (at 117 cm depth).

The reconstructed MAT ranges between 7.9 and 8.2°C in the lowest part of the record between 95 and 123 cm depth. It shows an increase to 8.6°C around 42 kyrBP (90 cm depth). It then drops back to 8.1 to 8.4°C until 36 kyrBP. The lowest MAT (7.9°C) is recorded at about 45 kyrBP (113 cm depth). Temperature around 8.7°C are recorded for the mid Holocene. After that, MAT increases rapidly to 8.9°C at about 3 kyrBP (45 cm). Throughout the late Holocene, the temperatures fluctuate between 8.3 and 9.2°C. The MAT reconstructed for the study sites is 9.6°C, which is close to today's temperature from the site of 10.1°C.

The reconstructed Tmin values vary between -1.1 and -0.4°C throughout the pre-LGM. At no point Tmin exceeds the frostline. In the mid and late Holocene fluctuates strongly between -1.5°C and + 0.5°C. The lowest Tmin is recorded in the late Holocene at 2.6 kyrBP (-1.2°C) and at about 1 ka (-1.5°C). In the mid and late Holocene the Tmin values frequently exceed the frostline. The Tmin reconstructed for the study site today is 1.1°C which is very close to the Tmin of 1.3°C observed at 2600 ma.s.l. today.

The PCA based on the WeruWeru pollen record revealed a first principle component (PC 1) reflecting 46.6% of the variation inherent in pollen record and a second principle component reflecting 25.4%. PC 1 is plotted next to the quantitative climate reconstruction (Fig. 5) to facilitate the detection and interpretation of past forest community and climate patterns. While during the pre-LGM the pollen taxa composition of the site seems to have been rather stable, the Holocene is characterized by major taxa composition changes and fast turnover rates indicated by a rapid change in standard deviation units of the first principle component.

Pollen-based temperature and precipitation inferences

L. Schüler et al.

Title Page

Abstract

Introduction

Conclusions

References

Tables

Figures

⏪

⏩

◀

▶

Back

Close

Full Screen / Esc

Printer-friendly Version

Interactive Discussion



Pollen-based temperature and precipitation inferences

L. Schüler et al.

Title Page	
Abstract	Introduction
Conclusions	References
Tables	Figures
⏪	⏩
◀	▶
Back	Close
Full Screen / Esc	
Printer-friendly Version	
Interactive Discussion	

of unpublished data of A. Hemp (600 forest relevées from Kilimanjaro) reveals that all these taxa have a unimodal distribution regarding abundance and biomass along the climatic gradient. Studies on pollen representivity have shown that despite pollen production and dispersal patterns the underlying vegetation composition can still be identified (Schüler, 2013).

Taxa such as *Podocarpus* and *Araliaceae* seem to have a rather narrow MAT optimum area whereas *Olea* and *Macaranga* are rather tolerant and display a broader temperature optimum. This unimodal response of taxa was further supported by the long environmental gradient revealed by the DCA. The CCA revealed that all the climate variables are important environmental factors influencing the distribution of the pollen taxa. In all ordinations, the explained variance in the pollen data set is high. The correlation between pollen taxa and the climate variables indicates a strong relationship between species and environment, which is supported by the permutation test results. Based on these outcomes, the quantitative inference models for these variables from the pollen assemblages were developed.

5.2 Model performance

The assessment of the pollen training subset selection and the WA-PLS model performance shows that the type of data transformation used plays an important role for the reconstruction. Skewed data and data with many rare or absent taxa are often transformed by taking the square-root (Legendre and Legendre, 2012). Since in our study not only the most abundant pollen taxa (e.g. *Ericaceae* and *Macaranga*) show a good correlation with MAP, MAT and Tmin but also taxa that have a low occurrence (e.g. *Olea*), square-root transformations amplify the weight of these taxa. The normalizing effect of the square-root transformation allows the selection of rare taxa into the subset and relativizes the effect of dominant taxa on the transfer function. Our results show that this is very important to consider when climate parameters are to be reconstructed from pollen taxa compositions instead of single taxa only. Data transformation facilitates rare taxa or the presents and absents of taxa, which can still act as discriminant



Pollen-based temperature and precipitation inferences

L. Schüler et al.

[Title Page](#)

[Abstract](#)

[Introduction](#)

[Conclusions](#)

[References](#)

[Tables](#)

[Figures](#)

[⏪](#)

[⏩](#)

[◀](#)

[▶](#)

[Back](#)

[Close](#)

[Full Screen / Esc](#)

[Printer-friendly Version](#)

[Interactive Discussion](#)

vegetation reconstructions from the Rukiga highlands in southwest Uganda (Taylor, 1990). In addition, contemporaneous records from Sacred Lake, Mt. Kenya (Coetzee, 1967; Olago, 2001) and Kamiranzovu Swamp (Hamilton, 1982) are in accordance with these results. The increase in shrubs and trees indicate a shift of vegetation zones to higher elevations suggest humid and comparatively warm climate conditions at Maundi Crater (Schüler et al., 2012). Based on Mt. Kilimanjaro temperature lapse rates varying from 0.51 to 0.56 °C per 100 m rise (Hemp, 2006b) the reconstructed temperatures at our study site at 2600 m of 7.9 to 8.2 °C translate into a vegetation shift of about 300 m during the late pre-LGM. This is more than Mumbi et al. (2008) reconstructed, who observe an altitudinal shift of montane forest from 1700 to 1800 m a.s.l. to 1800–1900 m a.s.l. in the Eastern Arc Mountains of Tanzania. However, this difference could be caused by the shadowing effect of the surrounding mountains in the Eastern Arc, which leads to less extreme climate conditions within in the mountains range compared to freestanding mountains as the Kilimanjaro. Hence, our MAT reconstruction reflects the decreasing temperature trend approaching the LGM. Lake Chala temperature reconstruction based on distributions of branched GDGTs infer LGM temperatures 7–10 °C lower than today (Sinninghe Damsté et al., 2012) which suggests that a rapid temperature decrease in the Kilimanjaro area occurred after 36 ka. Interesting is, that despite the MAT being slightly higher in the late pre-LGM compared to the early pre-LGM, the lowest T_{min} is reconstructed for the late pre-LGM. This suggests that in spite of the relatively moderate temperatures on average, the frequency and severity of low temperature events increased towards the LGM.

The pollen-based temperature and precipitation reconstruction from Kashiru Swamp at 2104 m a.s.l. in the Burundi Highlands, estimate the LGM climate being by 3–4 °C cooler and drier (ca. 30 % less rainfall) than today (Bonnefille and Chalié, 2000; Bonnefille et al., 1992). Such LGM temperatures would have caused a descent of vegetation zone on Mt. Kilimanjaro by another 300–400 m after the late pre-LGM. Recent vegetation reconstruction on Mt. Kilimanjaro suggest a vegetation shift of about 1000 m for the LGM (Schüler et al., 2012; Zech, 2006), which corresponds well with

Pollen-based temperature and precipitation inferences

L. Schüler et al.

[Title Page](#)

[Abstract](#)

[Introduction](#)

[Conclusions](#)

[References](#)

[Tables](#)

[Figures](#)

[⏪](#)

[⏩](#)

[◀](#)

[▶](#)

[Back](#)

[Close](#)

[Full Screen / Esc](#)

[Printer-friendly Version](#)

[Interactive Discussion](#)

LGM temperature decrease of 5.1 °C suggested for East African Lakes (Loomis et al., 2012). The lowering of temperatures during the LGM in East Africa decreased to 5–6 °C on average, which also matches the reduction of the SST's in the western Indian Ocean between 0° N and 20° S and west of 50° E (Anhuf, 2000). Results from other east African high mountains show that the overall lowering of the vegetation belts during the LGM amounted to ±700 m in the dry high mountains, whereas in the humid high mountains it amounted to ±1000 m (Coetzee, 1967; Hamilton, 1982; Perrott and Street-Perrott, 1982; Maitima, 1991; Olago et al., 2000).

Despite the assumed vegetation zone shifts during the pre-LGM the taxa composition within the prevailing vegetation remained rather stable as proposed by the ordination of the pollen taxa. The variations in MAT, Tmin and MAP had only a minor impact on the taxonomic structure of the montane plant communities during that time.

5.4 Holocene climate reconstruction

Precipitation and temperature fluctuate strongly throughout the Holocene. Mid and late Holocene MAT is between 0.4 and 1.4 °C lower than today. MAP is between 4 and 20 % lower than today and the Tmin exceed the frostline just after 6 ka for the first time in the record. This suggests increased unstable climate conditions throughout the Holocene, which is a common phenomenon in the tropics (Mayewski et al., 2004).

Our pollen-based reconstruction proposes very relatively warm and wet mid Holocene around 6 kyrBP). Heavy convective precipitation for around 6 kyrBP also is suggested by $\delta^{18}\text{O}_{\text{diatom}}$ from Lake Challa (Barker et al., 2011).

The Kilimanjaro ice core records reflect this substantial cooling between 6.5 to 5.2 kyrBP (Thompson et al., 2002) which cannot be derived from our results. Neither does can we observe the dry conditions assumed from pollen record of Maundi Crater, Kilimanjaro (Schüler et al., 2012) and hydrology reconstructions (BIT index) of Lake Challa at the foot of Mt. Kilimanjaro (Verschuren et al., 2009; Moernaut et al., 2010).

A second abrupt dry event picked up in our record around 2.5 kyrBP is also recorded from the Kilimanjaro ice cores as enhanced dust input and lowered $\delta^{18}\text{O}_{\text{ice}}$ (Thompson

existence of montane forests, even a minor reduction in precipitation over the past decades as observed by Hemp (2005) could already have a major effect on the vegetation.

In prospective studies, the quantitative climate reconstruction can be improved by additional modern pollen rain data, especially from lower elevations with submontane dry forests and colline savanna vegetation. It is unlikely that the temperature and precipitation patterns revealed by our record would be strongly modified since potential Late Glacial climate conditions are well covered by our modern pollen rain data set. However, warmer and especially drier phases would probably be refined since the climate gradient covered here does not span elevations < 1900 m a.s.l. (with higher temperatures and decreasing precipitation). Further, outlier samples, such as samples with unusual pollen assemblages or unusual combination of environmental variables, or a pollen assemblage with poor relationship to MAP and/or MAT can strongly affect the predictive power of transfer functions (Birks et al., 1990; Hall and Smol, 1992) or eventually the respective reconstruction. Hutson (1976) points out that failure of transfer functions due to environmental conditions that have no modern analogue may be cryptic, but that chances for discovery are increased if more than one transfer function algorithm is applied to a given set of samples. Moreover, it needs to be explored in more detail, which taxa are to be included, and how they are weighted in the calibration, and eventually influence the reconstruction.

Hence, there is an urgent need of modern pollen-rain studies in tropical East Africa in order to establish pollen–climate relationships that show a strong and stable correlation. This will strongly improve the model performances and lead to much better predictions of climate parameter variations based on fossil pollen distribution.

6 Conclusions

Studies of the Quaternary period, especially the period from the LGM onwards, have two great advantages: a wealth of accurately dated information, and the fact that very

Pollen-based temperature and precipitation inferences

L. Schüler et al.

Title Page

Abstract

Introduction

Conclusions

References

Tables

Figures

⏪

⏩

◀

▶

Back

Close

Full Screen / Esc

Printer-friendly Version

Interactive Discussion



**Pollen-based
temperature and
precipitation
inferences**

L. Schüler et al.

[Title Page](#)[Abstract](#)[Introduction](#)[Conclusions](#)[References](#)[Tables](#)[Figures](#)[Back](#)[Close](#)[Full Screen / Esc](#)[Printer-friendly Version](#)[Interactive Discussion](#)

little macroevolution or natural extinction has taken place on this time scale so that observed biotic transitions can be interpreted based on knowledge of the present-day biota. It is possible to compute pollen transfer functions relating the distribution of fossil pollen to the distribution of the climatic parameter of interest. However, this implies the existence of an adequate set of fossil samples and a representative training data set, hence, meaning good data on the distribution of environmental parameters under modern conditions. This relationship can then be used to estimate the climate values under past conditions. This computation is crucially dependent on a strong and stable correlation between climate parameter variations and fossil distribution. If these constraints are satisfied, the transfer functions derived through WA-PLS yield comparable results. The response of the pollen taxa to the climate variables differs between taxa. In our study, the majority of pollen taxa seems to follow a normal distribution along the elevation gradient recorded in this study are probably caused by the incomplete inventory of the climate gradient. The assessment of the WA-PLS model performance shows that the type of data transformation used plays an important role for the reconstruction. Our best-fit transfer function is the one based on square root -transformed modern pollen-rain data, which is subset individually for each reconstructed climate variable by forward selection. We can show that it is important to include the information inherent in rare taxa. These taxa should receive special attention and need to be reinforced prior to model application. The reconstructed climate patterns for our fossil pollen record from the afro-montane forest on Mt. Kilimanjaro are consistent with the interpretation of pollen data in terms of vegetation history of montane forest and with general climate trends during the past 45 kyrBP in tropical East Africa. The pre-LGM is characterized by a climate about 1.7 °C cooler and by about 25 % drier than today. Towards the LGM, the annual minimum temperatures decreased and showed more fluctuations despite mostly unchanging mean annual temperature and only slightly increased annual precipitation. Due to a hiatus, the LGM is missing in the record. During the mid and late Holocene, our reconstructions reveal warmer and particularly more

Pollen-based temperature and precipitation inferences

L. Schüler et al.

[Title Page](#)

[Abstract](#)

[Introduction](#)

[Conclusions](#)

[References](#)

[Tables](#)

[Figures](#)

[⏪](#)

[⏩](#)

[◀](#)

[▶](#)

[Back](#)

[Close](#)

[Full Screen / Esc](#)

[Printer-friendly Version](#)

[Interactive Discussion](#)

- Barker, P. A., Hurrell, E. R., Leng, M. J., Wolff, C., Cocquyt, C., Sloane, H. J., and Verschuren, D.: Seasonality in equatorial climate over the past 25 kyr revealed by oxygen isotope records from Mount Kilimanjaro, *Geology*, 39, 1111–1114, 2011.
- Bartlein, P. J., Webb III, T., and Fleri, E.: Holocene climatic change in the northern Midwest: pollen-derived estimates, *Quaternary Res.*, 22, 361–374, doi:10.1016/0033-5894(84)90029-2, 1984.
- Bartlein, P. J., Prentice, I. C., and Webb, T.: Climatic response surfaces from pollen data for some eastern North American taxa, *J. Biogeogr.*, 13, 35–37, 1986.
- Bartlein, P. J., Harrison, S. P., Brewer, S., Connor, S., Davis, B. A. S., Gajewski, K., Guiot, J., Harrison-Prentice, T. I., Henderson, A., Peyron, O., Prentice, I. C., Scholze, M., Seppä, H., Shuman, B., Sugita, S., Thompson, R. S., Viau, A. E., Williams, J., and Wu, H.: Pollen-based continental climate reconstructions at 6 and 21 ka: a global synthesis, *Clim. Dynam.*, 37, 775–802, doi:10.1007/s00382-010-0904-1, 2011.
- Battarbee, R. W.: Diatom analysis and the acidification of lakes, *Philos. T. R. Soc. B*, 305, 451–477, 1984.
- Birks, H. J. B.: Quaternary palaeoecology and vegetation science – current contributions and possible future developments, *Rev. Palaeobot. Palynol.*, 79, 153–177, 1993.
- Birks, H. J. B.: Quantitative paleoenvironmental reconstructions, in: *Statistical Modelling of Quaternary Science Data*, edited by: Maddy, D. and Brew, J. S., Quaternary Research Association, Cambridge, 161–254, 1995.
- Birks, H. J. B.: Numerical tools in palaeolimnology – progress, potentialities, and problems, *J. Paleolimnol.*, 20, 307–332, doi:10.1023/A:1008038808690, 1998.
- Birks, H. J. B., Line, J. M., Juggins, S., Stevenson, S., and ter Braak, C. J. F.: Diatoms and pH reconstruction, *Philos. T. R. Soc. B*, 327, 263–278, 1990.
- Birks, H. J. B., Heiri, O., Seppä, H., and Bjune, A. E.: Strength and weaknesses of quantitative climate reconstructions based on late quaternary biological proxies, *The Open Ecology Journal*, 3, 68–110, 2010.
- Bonnefille, R. and Chalié, F.: Pollen-inferred precipitation time-series from equatorial mountains, Africa, the last 40 kyr BP, *Global Planet. Change*, 26, 25–50, 2000.
- Bonnefille, R., Chalié, F., and Guiot, J., and Vincens, A.: Quantitative estimates of full glacial temperature in equatorial Africa from palynological data, *Clim. Dynam.*, 6, 251–257, 1992.

Pollen-based temperature and precipitation inferences

L. Schüler et al.

[Title Page](#)

[Abstract](#)

[Introduction](#)

[Conclusions](#)

[References](#)

[Tables](#)

[Figures](#)

[⏪](#)

[⏩](#)

[◀](#)

[▶](#)

[Back](#)

[Close](#)

[Full Screen / Esc](#)

[Printer-friendly Version](#)

[Interactive Discussion](#)

Cheddadi, R., Lamb, H. F., and Guiot, J., and van der Kaars, S.: Holocene climatic change in Morocco: a quantitative reconstruction from pollen data, *Clim. Dynam.*, 14, 883–890, doi:10.1007/s003820050262, 1998.

Coetzee, J. A.: Pollen analytical studies in east and southern Africa, in: *Palaeoecology of Africa and of the Surrounding Islands and Antarctica*, edited by: van Zindereren Bakker, E. M., Balkema, Cape Town, Amsterdam, 1–146, 1967.

Conolly, A. P.: 7. Some climatic and edaphic indications from the late-glacial flora, in: *Proceedings of the Linnean Society of London*, 172, 56–62, doi:10.1111/j.1095-8312.1961.tb00867.x, 1961.

Daniels, L. D. and Veblen, T. T.: Spatiotemporal influences of climate on altitudinal treeline in northern Patagonia, *Ecology*, 85, 1284–1296, 2004.

Faegri, K. and Iversen, J.: *Textbook of Pollen Analysis*, 4th edn., Wiley, Chichester, 1989.

Fritz, S. C., Juggins, S., Battarbee, R. W., and Engstrom, D. R.: Reconstruction of past changes in salinity and climate using a diatom-based transfer function, *Nature*, 352, 706–708, 1991.

Froyd, C. A. and Willis, K. J.: Emerging issues in biodiversity and conservation management: the need for a palaeoecological perspective, *Quaternary Sci. Rev.*, 27, 1723–1732, doi:10.1016/j.quascirev.2008.06.006, 2008.

Guiot, J.: Methodology of the last climatic cycle reconstruction in France from pollen data, *Methods for the Study of Stratigraphical Records*, 80, 49–69, doi:10.1016/0031-0182(90)90033-4, 1990.

Guiot, J. and Vernal, A. de: Chapter 13 transfer functions: methods for quantitative paleoceanography based on microfossils, in: *Developments in Marine Geology Proxies in Late Cenozoic Paleocyanography*, edited by: Hillaire–Marcel, C. and De Vernal, A., Elsevier, Amsterdam, 523–563, 2007.

Guiot, J., Pons, A., de Beaulieu, J. L., and Reille, M.: A 140 000 yr continental climate reconstruction from two European pollen records, *Nature*, 338, 309–313, doi:10.1038/338309a0, 1989.

Hall, R. I. and Smol, J. P.: A weighted-averaging regression and calibration model for inferring total phosphorus concentration from diatoms in British Columbia, *Freshwater Biol.*, 27, 417–434, 1992.

Hamilton, A. C.: *Environmental History of East Africa: A Study of the Late Quaternary*, Academic Press, London, 1982.

Pollen-based temperature and precipitation inferences

L. Schüler et al.

[Title Page](#)

[Abstract](#)

[Introduction](#)

[Conclusions](#)

[References](#)

[Tables](#)

[Figures](#)

[⏪](#)

[⏩](#)

[◀](#)

[▶](#)

[Back](#)

[Close](#)

[Full Screen / Esc](#)

[Printer-friendly Version](#)

[Interactive Discussion](#)

- Harrison, S. P., Prentice, I. C., Barboni, D., Kohfeld, K. E., Ni, J., and Sutra, J.-P.: Ecophysiological and bioclimatic foundations for a global plant functional classification, *J. Veg. Sci.*, 21, 300–317, doi:10.1111/j.1654-1103.2009.01144.x, 2010.
- Hemp, A.: Ecology of the pteridophytes on the southern slopes of Mt. Kilimanjaro. Part II: Habitat selection, *Plant Biol.*, 3, 493–523, 2001.
- Hemp, A.: Climate change-driven forest fires marginalize the impact of ice cap wasting on Kilimanjaro, *Glob. Change Biol.*, 11, 1013–1023, doi:10.1111/j.1365-2486.2005.00968.x, 2005.
- Hemp, A.: Continuum or zonation? Altitudinal gradients in the forest vegetation of Mt. Kilimanjaro, *Plant Ecol.*, 184, 27–42, 2006a.
- Hemp, A.: Vegetation of Kilimanjaro: hidden endemics and missing bamboo, *Afr. J. Ecol.*, 44, 305–328, doi:10.1111/j.1365-2028.2006.00679.x, 2006b.
- Holdridge, L. R.: *Life Zone Ecology*, rev. edn., Tropical Science Center, San Jose, Costa Rica, 206 pp., 1967.
- Huntley, B. and Prentice, I. C.: July temperatures in Europe from pollen data, 6000 yr BP, *Science*, 241, 687–690, doi:10.1126/science.241.4866.687, 1988.
- Huntley, B., Bartlein, P. J., and Prentice, I. C.: Climatic control of the distribution and abundance of beech in Europe and North America, *J. Biogeogr.*, 16, 551–560, doi:10.2307/2845210, 1989.
- Hutson, W. H.: *Transfer Functions Under Non-Analogue Conditions*, Brown University, Providence, RI, 1976.
- Imbrie, J. and Kipp, N. G.: A new micro-palaeontological method for quantitative paleoclimatology: application to a late Pleistocene Caribbean cote, in: *The Late Cenozoic Glacial Ages*, edited by: Turekian, K., Yale University Press, New Haven, 71–181, 1971.
- Jackson, S. T. and Williams, J. W.: Modern analogs in quaternary paleoecology: here today, gone yesterday, gone tomorrow? *Annu. Rev. Earth Pl. Sc.*, 32, 495–537, doi:10.1146/annurev.earth.32.101802.120435, 2004.
- Jongman, R. H. G., ter Braak, C. J. F., and Van Tongeren, O. F. R.: *Data Analysis in Community and Landscape Ecology*, Cambridge University Press, New York, N.Y, xxi, 299, 1995.
- Juggins, S.: *Rioja: Analysis of Quaternary Science Data*, R package version (0.8-4), available at: <http://cran.r-project.org/package=rioja>, 2012.
- Körner, C.: *Alpine Plant Life: Functional Plant Ecology of High Mountain Ecosystems*, Springer Verlag, Berlin, Germany, 2003.

**Pollen-based
temperature and
precipitation
inferences**

L. Schüler et al.

[Title Page](#)[Abstract](#)[Introduction](#)[Conclusions](#)[References](#)[Tables](#)[Figures](#)[⏪](#)[⏩](#)[◀](#)[▶](#)[Back](#)[Close](#)[Full Screen / Esc](#)[Printer-friendly Version](#)[Interactive Discussion](#)

- Larcher, W. and Bauer, H.: Ecological significance of resistance to low temperature, in: Physiological Plant Ecology I, edited by: Lange, O., Nobel, P., Osmond, C., and Ziegler, H., Encyclopaedia of Plant Physiology, Springer, Berlin Heidelberg, 403–437, 1981.
- Lauer, W.: Klimatische Grundzüge der Höhenstufen tropischer Gebirge, Innsbruck: 40, Deutscher Geographentag, 76–90, 1976.
- Legendre, P. and Legendre, L.: Numerical Ecology, 3rd edn., Elsevier, Amsterdam, London, 2012.
- Li, Y., Xu, Q., Liu, J., Yang, X., and Nakagawa, T.: A transfer-function model developed from an extensive surface-pollen data set in northern China and its potential for palaeoclimate reconstructions, *Holocene*, 17, 897–905, doi:10.1177/0959683607082404, 2007.
- Loomis, S. E., Russell, J. M., Ladd, B., Street-Perrott, F. A., and Sinninghe Damsté, J. S.: Calibration and application of the branched GDGT temperature proxy on East African lake sediments, *Earth Planet. Sc. Lett.*, 357, 277–288, doi:10.1016/j.epsl.2012.09.031, 2012.
- Lotter, A., Birks, H. J., Hofmann, W., and Marchetto, A.: Modern diatom, cladocera, chironomid, and chrysophyte cyst assemblages as quantitative indicators for the reconstruction of past environmental conditions in the Alps, I. climate, *J. Paleolimnol.*, 18, 395–420, doi:10.1023/A:1007982008956, 1997.
- Macdonald, G. M., Bennett, K. D., Jackson, S. T., Parducci, L., Smith, F. A., Smol, J. P., and Willis, K. J.: Impacts of climate change on species, populations and communities: palaeobiogeographical insights and frontiers, *Prog. Phys. Geog.*, 32, 139–172, doi:10.1177/0309133308094081, 2008.
- Maitima, M. J.: Vegetation response to climatic change in Central Rift Valley, Kenya, *Quaternary Res.*, 35, 234–245, 1991.
- Marchant, R., Cleef, A., Harrison, S. P., Hooghiemstra, H., Markgraf, V., van Boxel, J., Ager, T., Almeida, L., Anderson, R., Baied, C., Behling, H., Berrio, J. C., Burbridge, R., Björck, S., Byrne, R., Bush, M., Duivenvoorden, J., Flenley, J., De Oliveira, P., van Geel, B., Graf, K., Gosling, W. D., Harbele, S., van der Hammen, T., Hansen, B., Horn, S., Kuhry, P., Ledru, M.-P., Mayle, F., Leyden, B., Lozano-García, S., Melief, A. M., Moreno, P., Moar, N. T., Prieto, A., van Reenen, G., Salgado-Labouriau, M., Schäbitz, F., Schreve-Brinkman, E. J., and Wille, M.: Pollen-based biome reconstructions for Latin America at 0, 6000 and 18 000 radiocarbon years ago, *Clim. Past*, 5, 725–767, doi:10.5194/cp-5-725-2009, 2009.

**Pollen-based
temperature and
precipitation
inferences**

L. Schüler et al.

[Title Page](#)[Abstract](#)[Introduction](#)[Conclusions](#)[References](#)[Tables](#)[Figures](#)[⏪](#)[⏩](#)[◀](#)[▶](#)[Back](#)[Close](#)[Full Screen / Esc](#)[Printer-friendly Version](#)[Interactive Discussion](#)

- Markgraf, V., Webb, R. S., Anderson, K. H., and Anderson, L.: Modern pollen/climate calibration for southern South America, *Palaeogeogr. Palaeoclimatol.*, 181, 375–397, doi:10.1016/S0031-0182(01)00414-X, 2002.
- 5 Mayewski, P. A., Rohling, E. E., Curt Stager, J., Karlén, W., Maasch, K. A., David Meeker, L., Meyerson, E. A., Gasse, F., van Kreveland, S., Holmgren, K., Lee-Thorp, J., Rosqvist, G., Rack, F., Staubwasser, M., Schneider, R. R., and Steig, E. J.: Holocene climate variability, *Quaternary Res.*, 62, 243–255, doi:10.1016/j.yqres.2004.07.001, 2004.
- 10 Moernaut, J., Verschuren, D., Charlet, F., Kristen, I., Fagot, M., and de Batist, M.: The seismic-stratigraphic record of lake-level fluctuations in Lake Challa: hydrological stability and change in equatorial East Africa over the last 140 kyr, *Earth Planet. Sc. Lett.*, 290, 214–223, 2010.
- Müller, M. J.: *Handbuch ausgewählter Klimastationen der Erde*, Forschungsstelle Bodenerosion der Universität Trier, Trier, 1989.
- 15 Mumbi, C. T., Marchant, R., Hooghiemstra, H., and Wooller, M. J.: Late Quaternary vegetation reconstruction from the Eastern Arc Mountains, Tanzania, *Quaternary Res.*, 69, 326–341, doi:10.1016/j.yqres.2007.10.012, 2008.
- Nakagawa, T., Tarasov, P. E., Nishida, K., Gotanda, K., and Yasuda, Y.: Quantitative pollen-based climate reconstruction in central Japan: application to surface and Late Quaternary spectra, *Quaternary Sci. Rev.*, 21, 2099–2113, doi:10.1016/S0277-3791(02)00014-8, 2002.
- 20 Odum, E. P.: *Fundamentals of Ecology*, Saunders, Philadelphia, 1971.
- Olago, D. O.: Vegetation changes over palaeo-time scales in Africa, *Clim. Res.*, 17, 105–121, 2001.
- Olago, D. O., Street-Perrott, F. A., Perrott, R. A., Ivanovich, M., and Harkness, D. D.: Late Quaternary glacial-interglacial cycle of climatic and environmental change on Mount Kenya, Kenya, *J. Afr. Earth Sci.*, 29, 593–618, 1999.
- 25 Olago, D. O., Street-Perrott, F. A., Perrott, R. A., Ivanovich, M., Harkness, D., and Odada, E. O.: Long-term temporal characteristics of palaeomonsoon dynamics in equatorial Africa, *Global Planet. Change*, 26, 159–171, 2000.
- Overpeck, J. T., Webb III, T., and Prentice, I. C.: Quantitative interpretation of fossil pollen spectra: dissimilarity coefficients and the method of modern analogs, *Quaternary Res.*, 23, 87–108, doi:10.1016/0033-5894(85)90074-2, 1985.
- 30 Perrott, R. A. and Street-Perrott, F. A.: New evidence for a late Pleistocene wet phase in north intertropical Africa, *Palaeoecol. A.*, 14, 57–75, 1982.

**Pollen-based
temperature and
precipitation
inferences**

L. Schüler et al.

[Title Page](#)[Abstract](#)[Introduction](#)[Conclusions](#)[References](#)[Tables](#)[Figures](#)[⏪](#)[⏩](#)[◀](#)[▶](#)[Back](#)[Close](#)[Full Screen / Esc](#)[Printer-friendly Version](#)[Interactive Discussion](#)

- Pickett, E. J., Harrison, S. P., Hope, G., Harle, K., Dodson, J. R., Peter Kershaw, A., Colin Prentice, I., Backhouse, J., Colhoun, E. A., D'Costa, D., Flenley, J., Grindrod, J., Haberle, S., Hassell, C., Kenyon, C., Macphail, M., Martin, H., Martin, A. H., McKenzie, M., Newsome, J. C., Penny, D., Powell, J., Ian Raine, J., Southern, W., Stevenson, J., Sutra, J.-P., Thomas, I., van der Kaars, S., and Ward, J.: Pollen-based reconstructions of biome distributions for Australia, Southeast Asia and the Pacific (SEAPAC region) at 0, 6000 and 18000 ¹⁴C yr BP, *J. Biogeogr.*, 31, 1381–1444, doi:10.1111/j.1365-2699.2004.01001.x, 2004.
- Prentice, I. C., Bartlein, P. J., and Webb III, T.: Vegetation and climate change in eastern North America since the Last Glacial Maximum, *Ecology*, 72, 2038–2056, doi:10.2307/1941558, 1991.
- Prentice, I. C., Jolly, D., and BIOME 6000 participants: Mid-Holocene and glacial-maximum vegetation geography of the northern continents and Africa, *J. Biogeogr.*, 27, 507–519, doi:10.1046/j.1365-2699.2000.00425.x, 2000.
- Richardson, J. L. and Dussinger, R. A.: Palaeolimnology of mid-elevation lakes in the Kenyan Rift Valley, *Hydrobiologia*, 143, 167–174, 1986.
- Sachs, H. M., Webb III, T., and Clark, D. R.: Paleoeological transfer functions, *Annu. Rev. Earth Pl. Sc.*, 5, 159–178, 1977.
- Sakai, A. and Larcher, W.: Frost survival of plants: Responses and adaptation to freezing stress, *Ecological Studies*, 62, Springer-Verlag, Berlin, New York, 321 pp., 1987.
- Schüler, L.: Studies on Late Quaternary Environmental Dynamics (Vegetation, Biodiversity, Climate, Soils, Fire and Human Impact) on Mt. Kilimanjaro, Dissertation, GCBE – Göttingen Centre for Biodiversity and Ecology, University of Göttingen, Göttingen, 191 pp., 2013.
- Schüler, L., Hemp, A., Zech, W., and Behling, H.: Vegetation, climate and fire-dynamics in East Africa inferred from the Maundi crater pollen record from Mt. Kilimanjaro during the last glacial-interglacial cycle, *Quaternary Sci. Rev.*, 39, 1–13, 2012.
- Seppä, H., Birks, H. J. B., Odland, A., Poska, A., and Veski, S.: A modern pollen–climate calibration set from northern Europe: developing and testing a tool for palaeoclimatological reconstructions, *J. Biogeogr.*, 31, 251–267, doi:10.1111/j.1365-2699.2004.00923.x, 2004.
- Sinninghe Damsté, J. S., Ossebaar, J., Schouten, S., and Verschuren, D.: Distribution of tetraether lipids in the 25 kyr sedimentary record of Lake Challa: extracting reliable TEX86 and MBT/CBT palaeotemperatures from an equatorial African lake, *Quaternary Sci. Rev.*, 50, 43–54, doi:10.1016/j.quascirev.2012.07.001, 2012.

Pollen-based temperature and precipitation inferences

L. Schüler et al.

[Title Page](#)

[Abstract](#)

[Introduction](#)

[Conclusions](#)

[References](#)

[Tables](#)

[Figures](#)

[⏪](#)

[⏩](#)

[◀](#)

[▶](#)

[Back](#)

[Close](#)

[Full Screen / Esc](#)

[Printer-friendly Version](#)

[Interactive Discussion](#)

- Spellerberg, I. F.: Monitoring Ecological Change, Cambridge University Press, Cambridge, England, 1991.
- Stager, J. C. and Mayewski, P.: Abrupt early to mid-Holocene climatic transition registered at the Equator and the Poles, *Science*, 276, 1834–1836, doi:10.1126/science.276.5320.1834, 1997.
- 5 Taylor, D.: Late Quaternary pollen records from two Ugandan mires: evidence for environmental change in the Rukiga Highlands of southwest Uganda, *Palaeogeogr. Palaeocl.*, 80, 283–300, 1990.
- ter Braak, C. J. F. and Juggins, S.: Weighted averaging partial least square regression (WAPLS): an improved method for reconstructing environmental variables from species assemblages, *Hydrobiologia*, 269/270, 485–502, 1993.
- 10 ter Braak, C. J. F. and Šmilauer, P.: Canoco for Windows, Biometris – Plant Research International, Wageningen, the Netherlands, 1997.
- ter Braak, C. J. F. and Šmilauer, P.: CANOCO Reference Manual and CanoDraw for Windows User's Guide: Software for Canonical Community Ordination, Microcomputer Power, Ithaca, NY, USA, 2002.
- 15 Thompson, L. G., Mosley-Thompson, E., Davis, M. E., Henderson, K. A., Brecher, H. H., Zagorodnov, V. S., Mashiotta, T. A., Lin, P.-N., Mikhalneko, V. N., Hardy, D. R., and Beer, R.: Kilimanjaro Ice Core records: evidence of Holocene climate change in tropical Africa, *Science*, 298, 589–593, 2002.
- 20 Tierney, J. E., Russell, J. M., Huang, Y., Sinninghe Damsté, J. S., Hopmans, E. C., and Cohen, A. S.: Northern Hemisphere controls on tropical Southeast African climate during the past 60 000 yr, *Science*, 322, 252–255, 2008.
- Verschuren, D., Sinninghe Damsté, J. S., Moernaut, J., Kristen, I., Blauw, M., Fagot, M., Haug, G. H., and CHALLAGEA project members: Half-precessional dynamics of monsoon rainfall near the East African Equator, *Nature*, 462, 637–641, 2009.
- 25 Wake, D. B., Hadly, E. A., and Ackerly, D. D.: Biogeography, changing climates, and niche evolution: biogeography, changing climates, and niche evolution, *P. Natl. Acad. Sci. USA*, 106, 19631–19636, doi:10.1073/pnas.0911097106, 2009.
- 30 Walker, I. R., Mott, R. J., and Smol, J. P.: Allerød–Younger Dryas lake temperatures from midge fossils in Atlantic Canada, *Science*, 253, 1010–1012, 1991.
- Walter, H., Harnickell, E., and Mueller-Dombois, D.: Climate-diagram maps of the individual continents and the Ecological Climate Regions of the Earth, Springer, Berlin, 1975.

Pollen-based temperature and precipitation inferences

L. Schüler et al.

[Title Page](#)

[Abstract](#)

[Introduction](#)

[Conclusions](#)

[References](#)

[Tables](#)

[Figures](#)

[⏪](#)

[⏩](#)

[◀](#)

[▶](#)

[Back](#)

[Close](#)

[Full Screen / Esc](#)

[Printer-friendly Version](#)

[Interactive Discussion](#)

- Webb III, T. and Bryson, R. A.: Late and postglacial climatic change in the northern Midwest, USA: quantitative estimates derived from fossil pollen spectra by multivariate statistical analysis, *Quaternary Res.*, 2, 70–115, 1972.
- Whittaker, R. H., Levin, S. A., and Root, R. B.: Niche, habitat, and ecotope, *Am. Nat.*, 107, 321–338, 1973.
- Willis, K. J., Bailey, R. M., Bhagwat, S. A., and Birks, H. J. B.: Biodiversity baselines, thresholds and resilience: testing predictions and assumptions using palaeoecological data, *Trends Ecol. Evol.*, 25, 583–591, doi:10.1016/j.tree.2010.07.006, 2010a.
- Willis, K. J., Bennett, K. D., Bhagwat, S. A., and Birks, H. J. B.: 4°C and beyond: what did this mean for biodiversity in the past?, *Syst. Biodivers.*, 8, 3–9, doi:10.1080/14772000903495833, 2010b.
- Woodward, F. I. and Williams, B. G.: Climate and plant distribution at global and local scales, *Vegetatio*, 69, 189–197, doi:10.1007/BF00038700, 1987.
- Xu, Q., Xiao, J., Li, Y., Tian, F., and Nakagawa, T.: Pollen-based quantitative reconstruction of Holocene climate changes in the Daihai Lake Area, Inner Mongolia, China, *J. Climate*, 23, 2856–2868, doi:10.1175/2009JCLI3155.1, 2009.
- Zagwijn, W. H.: Aspects of the Pliocene and Early Pleistocene vegetation in the Netherlands, *Proefschrift-Leiden*, 1960, “Ernest van Aelst”, Maastricht, 3 pp., 1960.
- Zagwijn, W. H.: Reconstruction of climate change during the Holocene in western and central Europe based on pollen records of indicator species, *Veg. Hist. Archaeobot.*, 3, 65–88, doi:10.1007/BF00189928, 1994.
- Zech, M.: Evidence for Late Pleistocene climate change from buried soils on the southern slopes of Mt. Kilimanjaro, Tanzania, *Palaeo*, 242, 303–312, 2006.

Pollen-based temperature and precipitation inferences

L. Schüler et al.

[Title Page](#)

[Abstract](#)

[Introduction](#)

[Conclusions](#)

[References](#)

[Tables](#)

[Figures](#)

[⏪](#)

[⏩](#)

[◀](#)

[▶](#)

[Back](#)

[Close](#)

[Full Screen / Esc](#)

[Printer-friendly Version](#)

[Interactive Discussion](#)



Table 1. Summary of the CCA (first two axes) with the climate variables, mean annual precipitation (MAP), mean annual temperature (MAT) and absolute minimum temperature (Tmin).

Climate Variable		1st CCA axis	2nd CCA axis	Permutation test result
MAP	Eigenvalues	0.2493	0.2374	Pseudo-F: 2.4 $P = 0.002$
	Species-environment correlation	0.9361		
	Cumulative percentage variance of species data	16.59	32.38	
MAT	Eigenvalues	0.2512	0.2545	Pseudo-F: 2.4 $P = 0.002$
	Species-environment correlation	0.9604		
	Cumulative percentage variance of species data	16.71	33.65	
Tmin	Eigenvalues	0.2576	0.2565	Pseudo-F: 2.5 $P = 0.002$
	Species-environment correlation	0.9694		
	Cumulative percentage variance of species data	17.14	34.20	

Table 2. The pollen training subsets for the three climate variables derived from forward selection. Pollen taxa are given with their percentage contribution to the explanatory power of the complete subset. Pollen taxa with a contribution $\geq 20\%$ were included in the transfer functions.

MAP		MAT		Tmin	
Taxon	Contrib. (%)	Taxon	Contrib. (%)	Taxon	Contrib. (%)
Ericaceae	63.8	Ericaceae	65.1	<i>Ocotea</i>	74
<i>Hagenia</i>	45.4	<i>Ocotea</i>	61.7	Ericaceae	63
<i>Hypericum</i>	43.9	<i>Macaranga</i>	59.6	<i>Macaranga</i>	59.1
Mimosaceae	41.1	<i>Artemisia</i>	53.8	<i>Thunbergia</i>	47.6
<i>Ocotea</i>	39.6	<i>Hypericum</i>	42.6	Mimosaceae	45.7
<i>Artemisia</i>	34.5	Mimosaceae	40.1	<i>Artemisia</i>	45.4
<i>Olea</i>	32.9	Asteraceae	38.3	<i>Olea</i>	43.8
<i>Thunbergia</i>	27.6	<i>Olea</i>	38.1	<i>Hypericum</i>	33.9
<i>Pauridiantha</i>	25.8	<i>Thunbergia</i>	36.3	<i>Hagenia</i>	30.6
<i>Chaetacme</i>	25.6	<i>Hagenia</i>	35.7	Asteraceae	30
Piperaceae	24.9	<i>Begonia</i>	33.7	<i>Begonia</i>	29.9
<i>Macaranga</i>	24.6	Apocynaceae	26.5	<i>Podocarpus</i>	28
<i>Trema</i>	24.5	<i>Combretum</i>	26.5	<i>Aneilema</i>	24.7
<i>Agarista</i>	24.1	<i>Ehretia</i>	26.5	<i>Mussaenda</i>	24.7
<i>Phyllanthus</i>	24	<i>Strombosium</i>	26.5	Piperaceae	23.3
<i>Lythrum</i>	22.7	<i>Trichodesma</i>	26.5		
<i>Pterolobium</i>	22.3	<i>Lythrum</i>	25.4		
<i>Ilex</i>	22.2	<i>Prunus/Rubus</i>	23.9		
<i>Polysphaeria</i>	20.9	<i>Celtis</i>	21.4		
<i>Conyza</i>	20.6	<i>Cyphostemma</i>	21.1		
<i>Nuxia</i>	20.6	<i>Plantago</i>	21.1		
<i>Plumbago</i>	20	<i>Valeriana</i>	21.1		
<i>Viola</i>	20	<i>Aneilema</i>	21		
<i>Prunus/Rubus</i>	20	<i>Mussaenda</i>	21		
		<i>Podocarpus</i>	20		

Pollen-based temperature and precipitation inferences

L. Schüler et al.

Title Page

Abstract

Introduction

Conclusions

References

Tables

Figures

⏪

⏩

◀

▶

Back

Close

Full Screen / Esc

Printer-friendly Version

Interactive Discussion

Pollen-based temperature and precipitation inferences

L. Schüler et al.

[Title Page](#)

[Abstract](#)

[Introduction](#)

[Conclusions](#)

[References](#)

[Tables](#)

[Figures](#)

[⏪](#)

[⏩](#)

[◀](#)

[▶](#)

[Back](#)

[Close](#)

[Full Screen / Esc](#)

[Printer-friendly Version](#)

[Interactive Discussion](#)

Table 3. Values of Root Mean Square Error of Prediction (RSEMP), Squared correlation between bootstrap predicted and observed values (R^2) and Randomisation t test significance (p) are given for the reconstructed climate variables MAP, MAT and Tmin. Values are given for the different number of components calculated for the WA-PLS model. *** ($p < 0.001$) indicate the significant WA-PLS components as revealed by the randomized t test. The RMSEP units are mm for MAP and °C for MAT and Tmin.

WAPLS comp.	MAP			MAT			Tmin		
	RMSEP	R^2	p	RMSEP	R^2	p	RMSEP	R^2	p
Comp 1	318.59	0.68	***	1.15	0.79	***	1.17	0.87	***
Comp 2	367.83	0.59	0.72	1.14	0.79	0.41	1.15	0.88	0.14
Comp 3	422.01	0.51	0.99	1.13	0.81	0.25	1.57	0.87	0.81

Pollen-based temperature and precipitation inferences

L. Schüler et al.

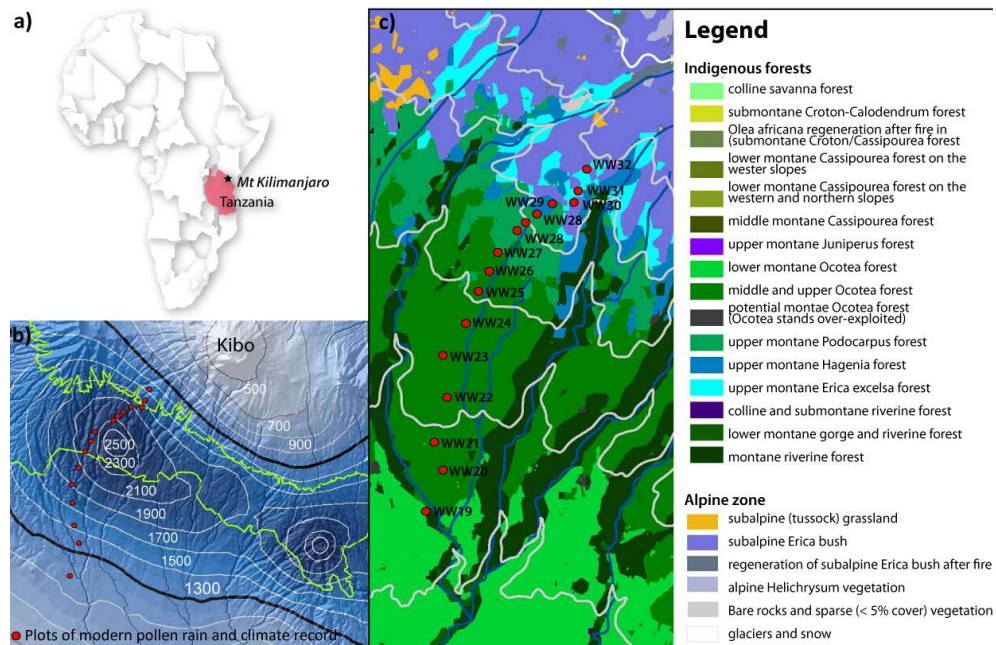


Fig. 1. (a) The study site Mt. Kilimanjaro in northern Tanzania. (b) Mean annual precipitation gradient on the southern slope of Mt. Kilimanjaro. Red circles indicate the WeruWeru transect sites, where the modern pollen-rain and the climate variables were recorded. (c) The vegetation types found on the southern slope of Mt. Kilimanjaro. Red circles indicate the WeruWeru transect sites.

Pollen-based
temperature and
precipitation
inferences

L. Schüler et al.

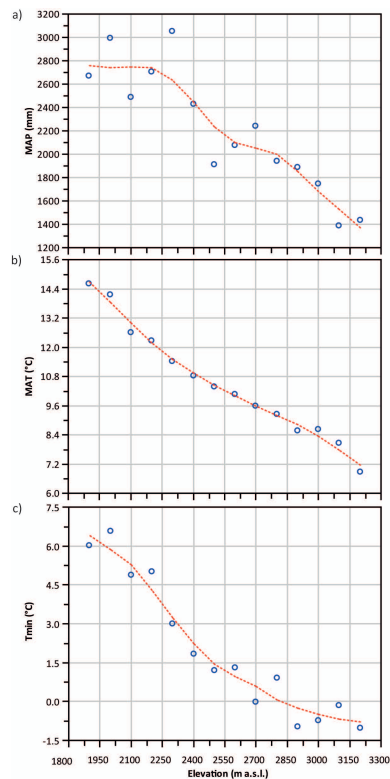


Fig. 2. Trend of mean annual precipitation (MAP), mean annual temperature (MAT) and absolute minimum temperature (Tmin) along the elevational gradient of the WeruWeru transect between 1900 and 3200 m a.s.l. on the southern slope of Mt Kilimanjaro. A local regression function (alpha: 0.45) was fitted to visualize the trend of the climate variables **(a)** MAP gradient **(b)** MAT gradient **(c)** Tmin gradient.

Pollen-based temperature and precipitation inferences

L. Schüler et al.

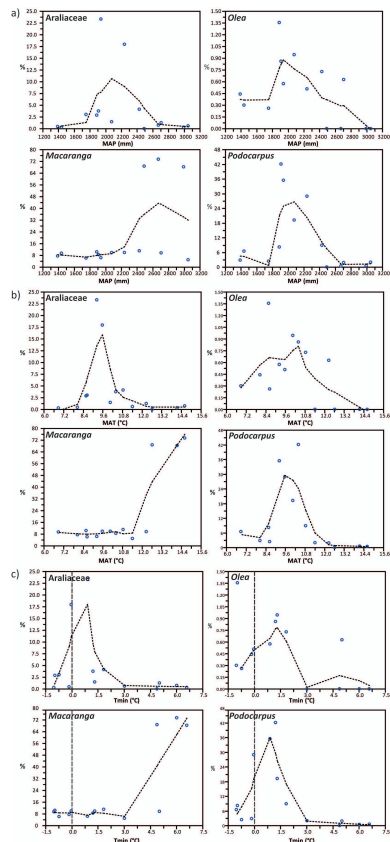


Fig. 3. Response curves of the pollen taxa to the climate variables mean annual temperature (MAT), mean annual precipitation (MAP) and along the WeruWeru transect between 1900 and 3200 ma.s.l. The taxa percentage at each site/elevation was plotted against the climate parameters measured at these sites. A local regression function (alpha: 0.45) was fitted to visualize the response trend **(a)** Taxa responses to MAP **(b)** Taxa responses to MAT.

Pollen-based temperature and precipitation inferences

L. Schüller et al.

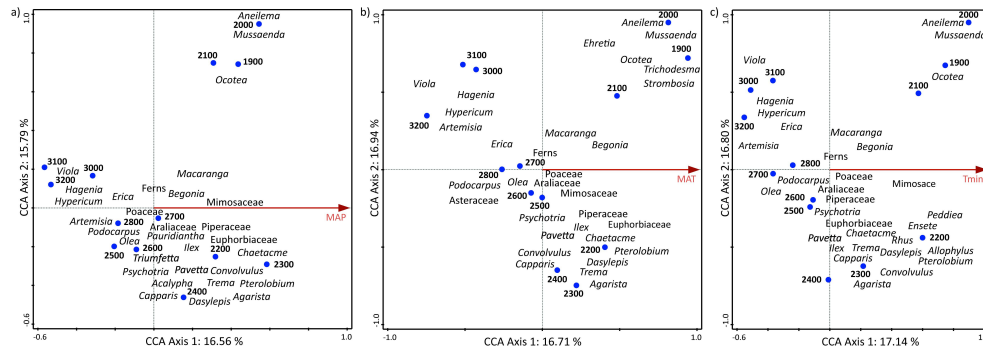


Fig. 4. Triplots of the Canonical Correspondence Analyses (CCA) of the modern pollen-rain data set from the WeruWeru transect, **(a)** CCA of the pollen taxa, the plots and the mean annual precipitation (MAP) as climate variable, **(b)** CCA of the pollen taxa, the plots and the mean annual temperature (MAT) as climate variable. The Eigenvalues are 0.2477 (CCA Axis 1) and 0.2465 (CCA Axis 2). The Eigenvalues are 0.2521 (CCA Axis 1) and 0.2270 (CCA Axis 2), **(c)** CCA of the pollen taxa, the plots and the absolute minimum temperature as climate variable. The Eigenvalues are 0.2508 (CCA Axis 1) and 0.2492 (CCA Axis 2).

Title Page

Abstract

Introduction

Conclusions

References

Tables

Figures

◀

▶

◀

▶

Back

Close

Full Screen / Esc

Printer-friendly Version

Interactive Discussion

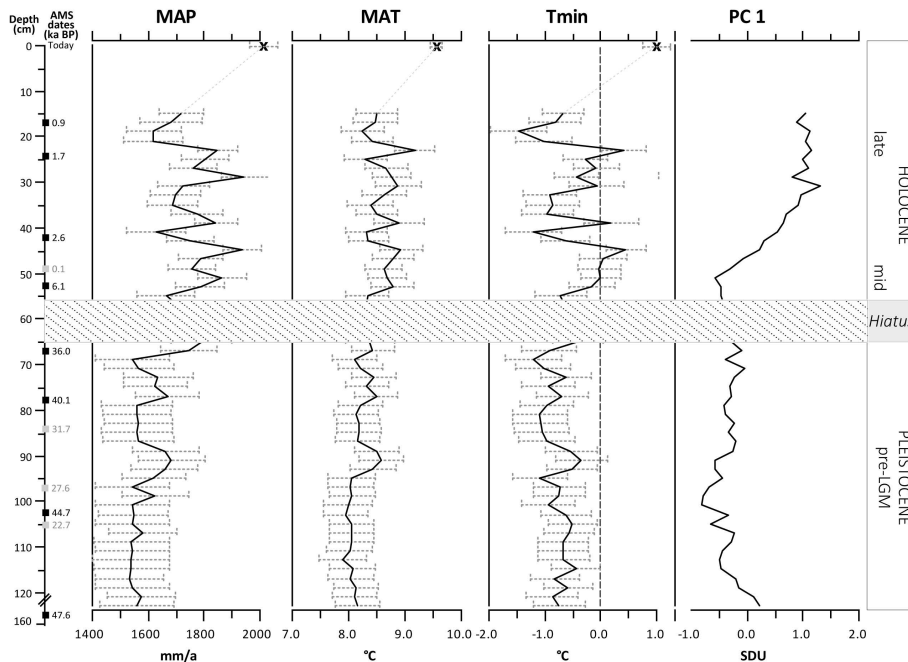


Fig. 5. Reconstruction of mean annual precipitation (MAP), mean annual temperature (MAT) and absolute minimum temperature (Tmin) of the WW26 pollen data set using weighted-averaging-least square regressions (WA-PLS). The error bars indicate the standard error of bootstrap estimated climate parameters of the correspondent WA-PLS component. For reference, the frost line is indicated in the Tmin graph (dashed grey line). AMS dates are given on the depth scale. The chronology suggests that the sediment above the hiatus (striated area) is part of the Holocene (ca 6–0 kyr) and sediment below the hiatus developed in the Late Glacial (47 to 36 kyr BP).